# Crystallization Kinetics of an Amorphous Pharmaceutical Compound Using Fluorescence-Lifetime-Imaging Microscopy

Rautaniemi, Kaisa

2018-05

Rautaniemi , K , Vuorimaa-Laukkanen , E , Strachan , C J & Laaksonen , T 2018 , ' Crystallization Kinetics of an Amorphous Pharmaceutical Compound Using Fluorescence-Lifetime-Imaging Microscopy ' , Molecular Pharmaceutics , vol. 15 , no. 5 , pp. 1964-1971 . https://doi.org/10.1021/acs.molpharmaceut.8b00117

http://hdl.handle.net/10138/301179
https://doi.org/10.1021/acs.molpharmaceut.8b00117

molecular pharmaceutics

Article

Cite This: Mol. Pharmaceutics 2018, 15, 1964−1971

# Crystallization Kinetics of an Amorphous Pharmaceutical Compound Using Fluorescence-Lifetime-Imaging Microscopy

Kaisa Rautaniemi,*[,†] Elina Vuorimaa-Laukkanen,[†] Clare J. Strachan,[‡] and Timo Laaksonen[†]

[†]Laboratory of Chemistry and Bioengineering, Tampere University of Technology, Korkeakoulunkatu 8, 33720 Tampere, Finland

[‡]Division of Pharmaceutical Chemistry and Technology, Faculty of Pharmacy, University of Helsinki, Viikinkaari 5 E, 00014 Helsinki, Finland

**ABSTRACT:** Pharmaceutical scientists are increasingly interested in amorphous drug formulations especially because of their higher dissolution rates. Consequently, the thorough characterization and analysis of these formulations are becoming more and more important for the pharmaceutical industry. Here, fluorescence-lifetime-imaging microscopy (FLIM) was used to monitor the crystallization of an amorphous pharmaceutical compound, indomethacin. Initially, we identified different solid indomethacin forms, amorphous and $\gamma$- and $\alpha$-crystalline, on the basis of their time-resolved fluorescence. All of the studied indomethacin forms showed biexponential decays with characteristic fluorescence lifetimes and amplitudes. Using this information, the crystallization of amorphous indomethacin upon storage in 60 °C was monitored for 10 days with FLIM. The progress of crystallization was detected as lifetime changes both in the FLIM images and in the fluorescence-decay curves extracted from the images. The fluorescence-lifetime amplitudes were used for quantitative analysis of the crystallization process. We also demonstrated that the fluorescence-lifetime distribution of the sample changed during crystallization, and when the sample was not moved between measuring times, the lifetime distribution could also be used for the analysis of the reaction kinetics. Our results clearly show that FLIM is a sensitive and nondestructive method for monitoring solid-state transformations on the surfaces of fluorescent samples.

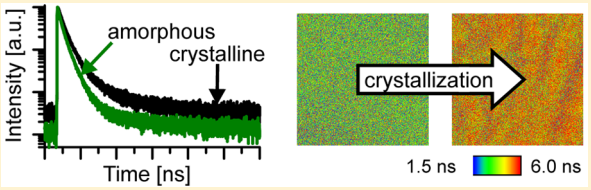


**KEYWORDS:** *fluorescence, fluorescence lifetime, amorphous materials, crystal growth, kinetics*



## INTRODUCTION

Poor water solubility and dissolution are major challenges in drug development. Most new drug candidates exhibit such behavior, which may result in poor oral bioavailability. A promising approach to solve this challenge is to utilize a drug's amorphous form, which lacks long-range molecular order and has different properties compared with its crystalline counterparts, including higher water solubility and a higher dissolution rate.[1,2] Unfortunately, the amorphous form is unstable and tends to crystallize into more stable crystalline forms. The crystallization can occur during the mechanical processing of the pharmaceutical product,[3] during storage,[4,5] or during dissolution.[6] The rate of crystallization depends on several factors, such as the method used to prepare the amorphous form,[6,7] the surface areas of the crystallizing particles,[8] and the storage conditions.[4,5]

Crystallization kinetics are traditionally monitored by X-ray powder diffraction (XRPD) and differential-scanning calorimetry (DSC).[2] Spectroscopic methods, including nuclear magnetic resonance[9] and Raman spectroscopy (FT-Raman[10] and low-frequency Raman[11]), are also used for quantifying amorphous contents in solid forms. Different methods observe the low percentages of crystalline or amorphous forms in samples differently. For example, a sample that appears completely amorphous when observed with XRPD might not be Raman- or DSC-amorphous.[12] Recently, fluorescence spectroscopy has been used for monitoring the crystallization of pure amorphous indomethacin.[13] Although fluorescence methods are mainly used for characterizing pharmaceuticals in solutions, they have also been utilized in solid-state contexts; the amounts of pharmaceuticals in tablet formulations have been estimated with fluorescence spectroscopy,[14−16] and fluorescence microscopy has been used to determine the miscibility of pharmaceutical-polymer solid dispersions.[17]

Fluorescence-lifetime-imaging microscopy (FLIM) is a method that maps the spatial distributions of excited-state lifetimes in microscopic samples. Therefore, it gives additional information compared with confocal or fluorescence microscopy. The fluorescence lifetime is an intrinsic property of the fluorescent molecule, and unlike fluorescence intensity, it does not depend on the concentration of the fluorophore in the sample; photobleaching; or issues related to the equipment, such as light scattering, the excitation intensity, or the sample's position. FLIM does not need high excitation intensities and is a noninvasive method; hence, it is used widely in biomedical applications.[18,19] FLIM has several advantages compared with traditional methods for monitoring crystallization. FLIM images show the distributions of lifetimes and fluorescence intensities in the sample, and therefore the method combines

Received: February 2, 2018
Revised: March 26, 2018
Accepted: March 27, 2018
Published: March 27, 2018

  

DOI: 10.1021/acs.molpharmaceut.8b00117
Mol. Pharmaceutics 2018, 15, 1964−1971

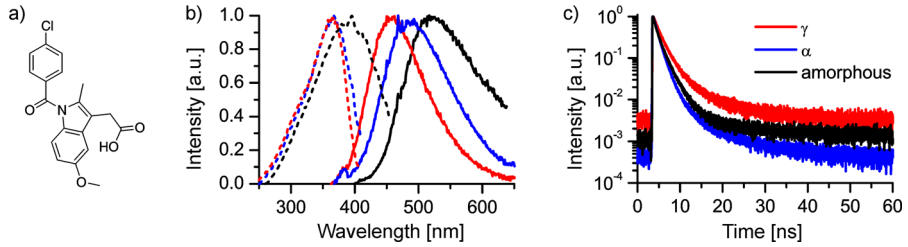


**Figure 1.** (a) Molecular structure of indomethacin. (b) Normalized excitation (dashed line) and emission (solid line) spectra for different forms of indomethacin. For the excitation spectra, the monitoring wavelengths were 460 ($\gamma$), 480 ($\alpha$), and 505 nm (amorphous). Fluorescence spectra were measured with an excitation at 340 nm. (c) Normalized fluorescence-decay curves measured by FLIM using an excitation at 405 nm. The fluorescence was monitored at 430–900 nm wavelengths. The decays were calculated from 30 × 30 $\mu$m areas for the crystalline forms and a 15 × 15 $\mu$m area for the amorphous form. The colors are the same in (b) and (c).

**Table 1. Thermal Properties for $\gamma$- and $\alpha$-Crystalline Indomethacin ($N$ = 2) and Amorphous Indomethacin ($N$ = 3)[a]**

| form | $T_g$ (°C) | $T_c$ (°C) | $T_m$ (°C) | $\Delta H_m$ (J g$^{-1}$ °C$^{-1}$) |
|---|---|---|---|---|
| $\gamma$ | — | — | 159.75 ± 0.02 | −109.30 ± 0.03 |
| $\alpha$ | — | — | 150.46 ± 0.09 | −90 ± 3 |
| amorphous | 44.6 ± 0.6 | 117 ± 5 | 156, 161 | −90 ± 5 |

[a]The glass-transition temperature, $T_g$ (midpoint); crystallization temperature, $T_c$ (onset); melting temperature, $T_m$ (onset); and melting enthalpy, $\Delta H_m$, were measured by DSC at a heating rate of 10 °C min$^{-1}$.

the advantages of spectral techniques and imaging techniques. As FLIM does not need high excitation intensities, it is less likely to destroy the sample with the excitation light than, for example, Raman spectroscopy.[10] The intrinsic nature of the fluorescence lifetime benefits quantitative analysis. Fluorescence lifetimes and their amplitudes are proportional to each other, even in situations when the fluorescence intensities might not be. For example, if the sample is moved, or the fluorescent pharmaceutical is unevenly distributed in a pharmaceutical product, the fluorescence intensity changes but the lifetime stays constant.

We now present the first attempt to monitor solid-state transformations quantitatively by fluorescence-lifetime-imaging microscopy. Indomethacin (Figure 1a), whose solid-state forms can be distinguished by their fluorescence,[13] was chosen as a model drug. Indomethacin is a nonsteroidal anti-inflammatory drug (NSAID) that has several well-characterized solid forms: the amorphous form and the $\alpha$- and $\gamma$-crystalline forms.[20] The $\gamma$-form is the most stable in ambient conditions, but amorphous indomethacin can crystallize to either of these two crystalline forms depending on the preparation method[7] and storage conditions.[4,5] We were able to identify amorphous and $\gamma$- and $\alpha$-crystalline indomethacin according to their time-resolved fluorescences. This information was used for following the crystallization of amorphous indomethacin upon storage. The progress of the crystallization was seen in the FLIM images and the fluorescence-decay curves as lifetime changes, and the decay data was used for a quantitative analysis of crystallization. Amorphous indomethacin was also crystallized rapidly with a drop of ethanol. In this arrangement, the sample was not moved between measurements. Thus, the intensities of the FLIM images were proportional to each other, and the progress of crystallization could be followed from the fluorescence-lifetime distributions.

## EXPERIMENTAL SECTION

**Materials.** Indomethacin (Orion Finland) was obtained in the $\gamma$-crystalline form and used as received. The amorphous form was obtained by melting $\gamma$-indomethacin on a glass microscope slide or aluminum pan at 175 °C on a heating plate. The completely melted indomethacin was cooled down at room temperature on a metallic surface for a few minutes and then transferred to a desiccator. Amorphous indomethacin was stored over NaOH (0% relative humidity, RH) in a desiccator for at least an hour before further treatment. $\alpha$-Indomethacin was prepared from $\gamma$-indomethacin dissolved in ethanol, using a recrystallization method modified from the method used by Kaneniwa et al.[21] as follows. A saturated indomethacin ethanol solution at 80 °C was quickly added to room temperature water. Indomethacin crystallized immediately. The crystals were removed by filtration and dried over NaOH in a desiccator for at least 24 h.

The different indomethacin forms were characterized by differential-scanning calorimetry (DSC, Mettler Toledo DSC821e). The samples (2.7–3.5 mg) were heated from 10 to 180 °C at 10 °C min$^{-1}$. The DSC results are presented in Table 1. The melting points and enthalpies for $\gamma$- and $\alpha$-indomethacin were similar to those published in the literature.[22,23] The amorphous form showed a glass-transition temperature around 45 °C, a crystallization exotherm, and two endothermic melting peaks, which correspond to the melting of $\alpha$- and $\gamma$-crystalline indomethacin. The DSC results for amorphous indomethacin are consistent with other studies.[6,7,24] The calibration of the DSC equipment was checked with an indium calibration sample.

**Monitoring Crystallization.** Fresh amorphous samples were stored in a desiccator at room temperature at 0% RH maintained by NaOH. For the simulated-storage experiment, four fresh amorphous samples were prepared on glass microscope slides. The intrinsic crystallization of the samples in the storage conditions, 60 °C and 0% RH, was monitored by FLIM for 10 days. Two of the freshly prepared samples were measured to represent $t$ = 0 before the samples were subjected to the storage conditions. Because one measurement sequence took about 1 h, two of the samples were measured after 3 h of storage at 60 °C and 0% RH, and the two other samples were measured after 6 h of storage. After that, three of the previous samples were chosen and these samples were measured at every


DOI: 10.1021/acs.molpharmaceut.8b00117
Mol. Pharmaceutics 2018, 15, 1964–1971

Table 2. Fluorescence Lifetimes, $\tau_i$; Amplitudes, $a_i$; and Excitation and Emission Maximum Wavelengths, $\lambda_{ex,max}$ and $\lambda_{em,max}$, of the Studied Indomethacin Forms[a]

| form | $\tau_1$ (ns) | $a_1$ | $\tau_2$ (ns) | $a_2$ | $\lambda_{ex,max}$ (nm) | $\lambda_{em,max}$ (nm) |
|---|---|---|---|---|---|---|
| $\gamma$ | 1.66 ± 0.02 | 0.93 | 6.2 ± 0.3 | 0.07 | 365 | 460 |
| $\alpha$ | 1.19 ± 0.01 | 0.97 | 5.2 ± 0.3 | 0.03 | 370 | 490 |
| amorphous | 1.07 ± 0.06 | 0.79 | 2.7 ± 0.2 | 0.21 | 395 | 520 |

[a]The time-resolved fluorescence data was measured by FLIM using excitation at 405 nm and monitoring the fluorescence at 430–900 nm wavelengths. The time-resolved fluorescence for each indomethacin form is presented as an average of 10 parallel FLIM images. The decay curves were extracted from 30 × 30 $\mu$m areas of FLIM images for the crystalline forms and a 15 × 15 $\mu$m area for the amorphous form. Excitation maxima were measured by monitoring wavelengths of 460 nm ($\gamma$), 480 nm ($\alpha$), and 505 nm (amorphous), and fluorescence maxima were measured using excitation at 340 nm.

time point. Three FLIM images representing the different samples for each time point were chosen for the analysis.

Crystallization was also induced by adding a drop of ethanol to the microscope slide and placing a fragment of amorphous indomethacin on top of the ethanol droplet. Crystallization was thus induced between the microscope slide and indomethacin fragment, which enabled the imaging of the crystallizing surface of the sample. Ethanol-induced crystallization was monitored for 95 min. The sample was not moved between imaging points in order to avoid external factors (e.g., the focal plane or imaged area) affecting the fluorescence intensity.

**Fluorescence Properties.** The fluorescence and excitation spectra were measured with a Fluorolog Yobin Yvon-SPEX spectrofluorometer (Horiba Scientific) for all of the indomethacin forms. A solid sample was pressed between two glass slides, and its emission was measured at a 20° angle relative to the excitation light (front-face geometry). The monitoring wavelengths for the excitation spectra were 505 nm ($\gamma$), 480 nm ($\alpha$), and 460 nm (amorphous). The excitation wavelength for the emission spectra was 340 nm for all the indomethacin forms.

The FLIM measurements were performed with a MicroTime 200 (PicoQuant) fluorescence-lifetime microscope coupled to an inverted Olympus IX-71 (Olympus) microscope. The samples were imaged with a 100× oil objective (numerical aperture, NA = 1.4) or a 40× air objective (NA = 0.65). A pulsed diode laser LDH-P-C-405 (PicoQuant) emitting at 405 nm with a 60 ps resolution was used for the fluorescence excitation. The maximum scan area of the equipment was 80 × 80 $\mu$m, and the spatial resolution was approximately 300 nm. For the present samples, the estimated laser-penetration depth was 500 nm. SymPhoTime version 4.7 software was used to calculate the lifetime-map images. The lifetime analyses were calculated using the whole FLIM image or smaller areas (the regions of interest, ROIs) if the fit was clearly better for the smaller area (for amorphous indomethacin) or if there were regions with different lifetimes in the same image. The fluorescence lifetimes, $\tau_i$, and their amplitudes, $a_i$, were calculated by the iterative least-squares tail-fitting method, in which the sums of the exponentials (eq 1) were fitted to the experimental-decay curves.

$$I(t) = \sum_{i=1}^{N} a_i e^{-t/\tau_i} \quad (1)$$

The quality of the fit was evaluated in terms of the weighted-mean-square-deviation $\chi^2$-test. The intensity-modulated FLIM images showed both the fluorescence-lifetimes and intensity distributions in the image. The FLIM images without intensity modulation showed only the lifetimes.

**Kinetic Analysis from Fluorescence Data.** The fluorescence lifetimes and their amplitudes were first determined for pure crystalline and amorphous samples, and these lifetimes were used as controls for determining the crystallinities of the stored samples. The time-resolved fluorescence of each pure form was calculated as an average of 10 parallel FLIM images. For the kinetic analysis, the degree of conversion, $\alpha$, was calculated by[25]

$$\alpha = \frac{a_0 - a_t}{a_0 - a_\infty} \quad (2)$$

where $a_0$ is the fluorescence-lifetime amplitude at $t = 0$, $a_t$ is the amplitude at $t$, and $a_\infty$ is the amplitude when the crystallization is complete.

For the ethanol-induced crystallization, the conversion was calculated by the changes in the lifetime distributions. The intensity at 1.74 ns, $I_a$, was assumed to correspond to the proportion of the amorphous form, and the intensity at 2.21 ns, $I_c$, was assumed to correspond to that of the crystalline form. Thus, the initial degree of conversion $\alpha'$ was calculated as

$$\alpha' = \frac{I_c}{I_a + I_c} \quad (3)$$

The shape and intensity of the fluorescence-lifetime distribution depends on the focal plane, sample distribution, and imaged area. Exact reproducibility for fluorescence-lifetime distributions is difficult, and the lifetime distributions of the pure samples could not be used as controls. The first FLIM image at $t = 5$ min was chosen to be $\alpha = 0$. The ethanol had not completely evaporated from the sample during the first few minutes, which supports us choosing $t = 5$ min as the onset of crystallization instead of $t = 0$. Because the crystallization was not complete at $t = 95$ min, the degree of conversion at the end of the monitoring period was estimated according to eq 2 with the fluorescence decays extracted from the FLIM-image areas where the conversion was clearest. $\alpha'$ was normalized between this value and 0 to obtain the degree of conversion.

## RESULTS AND DISCUSSION

Amorphous indomethacin and $\alpha$-indomethacin were prepared from $\gamma$-indomethacin as described above in the Experimental Section. The purities of the studied indomethacin forms were checked via their thermal properties, and they were further characterized spectroscopically. Both the steady-state and time-resolved fluorescences were distinctive for each of the forms (Table 2). The excitation and emission spectra are shown in Figure 1b. The excitation spectra were highly overlapping for the crystalline indomethacin forms, with an excitation maximum at around 370 nm, and the excitation spectrum for amorphous indomethacin was shifted to longer wavelengths,



DOI: 10.1021/acs.molpharmaceut.8b00117
Mol. Pharmaceutics 2018, 15, 1964–1971

with a maximum at 395 nm. The fluorescence maximum of $\alpha$-indomethacin was red-shifted by 30 nm, and the fluorescence maximum of amorphous indomethacin was red-shifted by 60 nm compared with that of $\gamma$-indomethacin, which were in agreement with previous studies.[13] The spectra for the crystalline forms were narrower than that of the amorphous form, which indicated a greater level of order. The amorphous form exhibited more intra- and intermolecular conformational variation and had more vibrational modes, which were seen as the broader spectrum.

The time-resolved fluorescence properties were measured by FLIM. All of the measured indomethacin forms showed biexponential fluorescence decays (Figure 1c) because of the different indomethacin isomers and hydrogen-bonding patterns in the solid states.[20,26−28] The fluorescence lifetimes, $\tau_1$ and $\tau_2$, and their amplitudes, $a_1$ and $a_2$, calculated by biexponential fits, are presented in Table 2. The shorter-lived component lasted between 1 and 2 ns for all the indomethacin forms. The longer lifetime was 5−6 ns for the crystalline forms and less than 3 ns for the amorphous indomethacin. The less-ordered structure leads to the excited states in the amorphous form decaying via vibrational relaxation more often than those in the crystalline forms, which shortens their lifetimes compared with those of the crystalline counterparts. Although the indomethacin forms could be identified by their varying lifetimes, the change in amplitudes between the amorphous and crystalline forms was more distinct and reliable. The amplitudes for the shorter lifetimes were 0.93 ($\gamma$) and 0.97 ($\alpha$) for the crystalline forms and 0.79 for the amorphous form. Therefore, changes in amplitude were used to represent the degree of crystallinity in the sample.

The different indomethacin forms could be distinguished from each other in the FLIM images, as seen in Figure 2. It is important to note that the images in Figure 2 are the raw images, and they display the average arrival time of the fluorescence photons after the excitation pulse at each pixel. Thus, the lifetime distributions differ somewhat from the fitted lifetimes. However, these images also provide the best contrast between the different forms of indomethacin and are thus utilized to visualize the crystallization processes. The color scale in Figure 2 visualizes the $\gamma$-crystalline form as red, the $\alpha$-crystalline as blue, and the amorphous form as green. In the partly crystalline image in Figure 2, the $\gamma$-crystalline form (bright red area) is clearly observed in the middle of the surrounding amorphous indomethacin.

On the basis of these results, it was concluded that the crystalline and amorphous forms of indomethacin could be differentiated in the FLIM images on the basis of their distinctive fluorescence lifetimes and amplitudes.

**Crystallization during Storage.** Next, the potential of the method to follow the crystallization of indomethacin during simulated storage conditions was investigated. This is a more complex system than that of the pure components studied above, as changes in storage can be fairly gradual, and detecting low levels of crystallinity is both important and challenging. To facilitate the detection of crystallization, crystallization was accelerated by storing the initially amorphous samples at an elevated temperature.

The crystallization of amorphous indomethacin at 60 °C and 0% RH was monitored for 10 days with FLIM. Thus, amorphous indomethacin samples were stored in a rubbery state, above their glass-transition temperature, $T_g$ (ca. 45 °C[29]). In these conditions, indomethacin has been reported to crystallize completely in 50 days.[4] As we were interested in detecting the early stages of crystallization, a 10 day monitoring period was considered sufficient. The surfaces of the samples appeared to be partially covered by a crystalline layer after 24 h and almost completely covered after 48 h when observed via optical microscopy (Figure 3). This rapid surface crystallization above $T_g$ is characteristic for $\gamma$-indomethacin crystallization.[30] During the rest of the storage period, the visual appearances of the samples changed only slightly. When monitored with FLIM, the changes in the samples during storage were more distinct than when they were monitored by optical microscopy, as seen in Figure 4. During the first few hours, the samples still resembled fresh amorphous indomethacin. As the crystalline

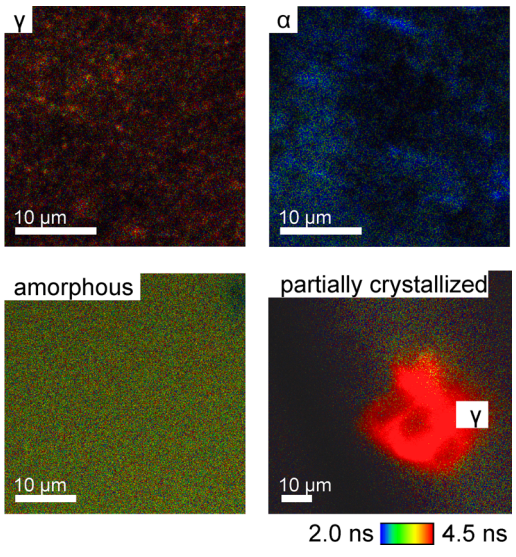


**Figure 2.** FLIM images of $\gamma$- and $\alpha$-crystalline, amorphous, and partially crystallized amorphous indomethacin. Images were taken using 100× magnification and oil immersion (for the pure indomethacin forms) or 40× magnification and air immersion (for the partially crystallized sample). The excitation wavelength was 405 nm, and the fluorescence was monitored at 430−900 nm wavelengths. The color scale for the fluorescence lifetimes is the same in all the images and is presented at the bottom right.

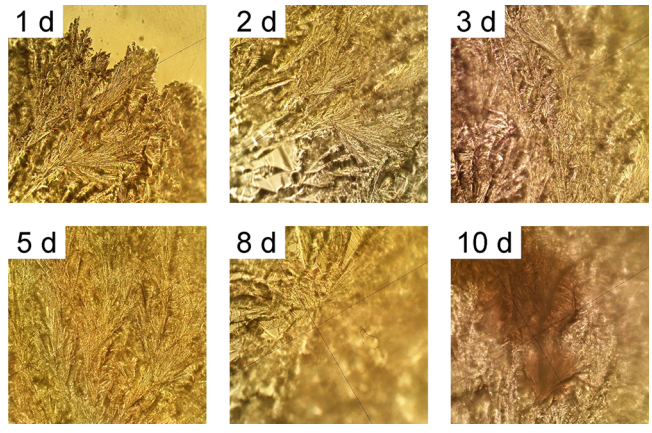


**Figure 3.** Optical-microscope images of the amorphous indomethacin samples stored at 60 °C and 0% RH for 10 days. The samples were imaged with 40× magnification and air immersion. The sizes of the images are approximately 300 × 300 $\mu$m.



DOI: 10.1021/acs.molpharmaceut.8b00117
Mol. Pharmaceutics 2018, 15, 1964−1971

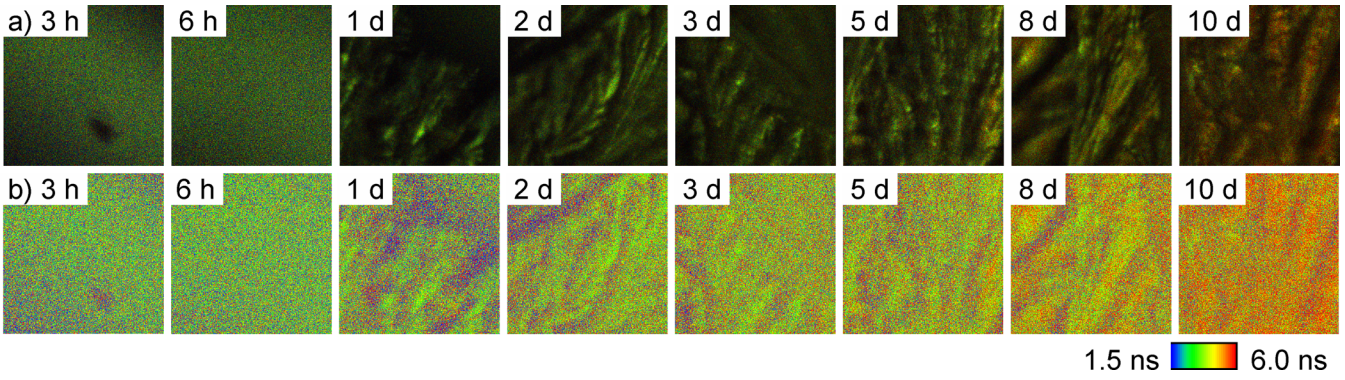


**Figure 4.** FLIM images (80 × 80 $\mu$m) of the amorphous indomethacin stored at 60 °C and 0% RH for 10 days. The same FLIM images are presented with (a) and without (b) intensity modulation. The images were taken with 40× magnification and air immersion. The excitation wavelength was 405 nm, and the fluorescence was monitored at 430−900 nm wavelengths. The color scale for the fluorescence lifetimes is the same in all the images and is presented at the bottom right.

layer started to cover the sample surfaces, the surfaces became uneven, which was also reflected in the FLIM images. The area of the sample in the focal plane has a higher fluorescence intensity than the areas outside the focal plane (Figure 4a), and the areas with low fluorescence intensities are tinged blue in the FLIM images without intensity modulation (Figure 4b).

As the crystallization proceeded, the colors in the FLIM images changed to be more red, which indicated longer lifetimes. The color change was not strictly located in specific areas, nor did it follow specific morphologies. Although the crystalline layer covered the samples quickly, the changes in the FLIM images were more subtle during the first few days. This indicated that the crystalline layers covering the samples were very thin, and the majority of the fluorescence signals in the FLIM images originated from the amorphous material under the crystalline layers. As the crystallization proceeded, the thicknesses of the crystalline layers increased, and the proportion of the fluorescence from amorphous material decreased.

The fluorescence-decay curves extracted from the FLIM images in Figure 4 are mixtures of the decay curves of pure amorphous and $\gamma$-crystalline indomethacin. The fluorescence decays of the pure forms (Figure 1c) and the lifetimes calculated from them (Table 2) are close to each other. Therefore, a four-exponential fit with fixed lifetimes for both the amorphous and $\gamma$-indomethacin did not give a reasonable result, and a biexponential fit was used instead. The obtained fluorescence lifetimes as a function of time are presented in Figure 5a. In the beginning, the lifetimes ($\tau_1$ = 1.03 ± 0.02 ns and $\tau_2$ = 2.57 ± 0.04 ns) clearly corresponded to amorphous indomethacin (Table 2).

Both $\tau_1$ and $\tau_2$ increased closer to the $\gamma$-indomethacin values as the crystallization progressed. After 10 days, $\tau_1$ was 1.48 ± 0.05 ns, and $\tau_2$ was 5.41 ± 0.11 ns. The amplitudes of the decay components changed during the crystallization process as well: the amplitude of $\tau_1$ ($a_1$) increased, and that of $\tau_2$ ($a_2$) decreased as the sample crystallized. At $t$ = 0, $a_1$ was 0.74, and after 10 days, it was 0.90. Because of the nature of the amorphous form, the amplitude values at $t$ = 0 differed somewhat from the values presented in Table 2 for amorphous indomethacin. Regardless, the freshly prepared samples were clearly amorphous at the beginning of the monitoring period. The change in amplitude was rapid in the beginning of the experiment and slowed down gradually as the crystallization proceeded, describing the progress of crystallization. The degree of conversion, $\alpha$, was

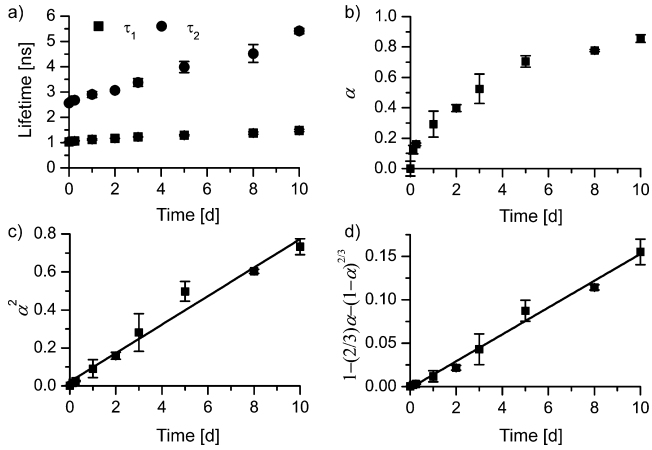


**Figure 5.** (a) Fluorescence lifetimes, $\tau_1$ and $\tau_2$, obtained from the biexponential fits to the decay curves extracted from the FLIM images; (b) degree of conversion, $\alpha$, calculated from the amplitude of the longer living component, $a_2$; (c) fit to the one-dimensional diffusion-limited reaction model (eq 4); and (d) fit to the three-dimensional diffusion-limited reaction model (eq 5) for the amorphous indomethacin samples stored at 60 °C and 0% RH for 10 days. $N$ = 2 for $t$ = 0 and $N$ = 3 for the other time points.

calculated from $a_2$ according to eq 2,[25] where $a_0$ was the $a_2$ value at $t$ = 0 and $a_\infty$ was the $a_2$ value determined for pure $\gamma$-indomethacin (Table 2). The degrees of conversion at different times during storage are presented in Figure 5b.

The crystallization of indomethacin is usually consistent with the Johnson−Mehl−Avrami−Erofeyev−Kolmogorov (JMAEK) model.[4,5,11,13,31] This model assumes that the crystallization process has two distinct steps, nucleation and growth, and the conversion forms a sigmoidal curve as a function of time. The shape of the conversion in this study is clearly not sigmoidal, and the JMAEK-model does not describe the kinetics of the monitored crystallization process. Hence, the present results were fitted to several decelerating kinetic models described by Kwaham et al.[25] The best agreement with our data was obtained with the diffusion-controlled models. In diffusion-controlled crystallization, the rate of the reaction decreases as the crystallized layer on the surface of a film or particle increases. For a one-dimensional reaction model, the reaction is assumed to occur on an infinite flat surface. In this case, the degree of conversion is directly proportional to crystalline-layer thickness, and the reaction model is written as


DOI: 10.1021/acs.molpharmaceut.8b00117
Mol. Pharmaceutics 2018, 15, 1964−1971

$$\alpha^2 = kt \quad (4)$$

where $k$ is a constant, and $t$ is time. The three-dimensional diffusion-controlled model is based on Fick's first law for radial diffusion in a sphere. The model is expressed as

$$1 - \frac{2}{3}\alpha - (1 - \alpha)^{2/3} = kt \quad (5)$$

and is known as the shrinking-core reaction model. The shrinking-core model is based on the assumption that the crystallizing particles are spherical and that crystallization starts at the surface of the particle. The limiting step in both models is the diffusion of the reagent through the production layer to the unreacted part of the sample.

The conversion is fitted to these models, and the fits are presented in Figure 5c,d (one-dimensional, $R^2$ = 0.973, and three-dimensional, $R^2$ = 0.987, respectively). The three-dimensional model gave the best fit, especially at the beginning of the crystallization process. However, there is no clear physical explanation for this result. Three-dimensional diffusion models are found to describe heterogeneous processes such as hydrate formation[32,33] and dissolution kinetics[34] but not usually crystallization from an amorphous phase. As the samples were single, solid amorphous pieces on microscope slides, it is unlikely that the sample would consist of spherical crystallizing particles. The one-dimensional crystallization model describing the thickening of the crystalline layer on an infinite plane is more consistent with the visual observation of the crystallization process, even though the fit to this model is not quite as good as that to the three-dimensional diffusion-controlled model. Although the samples were stored in the 0% RH desiccator, they were exposed to humidity regularly during measurements. Water is known to enhance molecular mobility and thus the crystallization rate in the amorphous form,[5] so it is possible that the model describes the reaction kinetics limited by the diffusion of water through the crystalline layer.

The observed crystallization occurred mostly on the sample surface, so the degree of crystallization for the whole sample was still low at the end of the monitoring period. Some amorphous-forming organic molecules, including indomethacin, are found to have different crystallizing mechanisms on the surface and in the bulk.[30,35,36] Surface crystallization is usually faster, and even a very thin crystalline layer on an otherwise amorphous material can affect the solubility and dissolution properties of the product.[37] In this study, we detected crystallization on the sample surface quantitatively and were able to follow the rate of crystalline-layer thickening.

**Ethanol-Induced Crystallization.** In the storage study above, the samples were measured at different times and stored in a desiccator between measurements. This means that the fluorescence intensity varied slightly from one measurement to the next. This was not an issue here and actually showed one of the benefits of following the fluorescence lifetime instead of the intensity. The lifetime is not dependent on the intensity. Therefore, we did not need to pay attention to having the same sample orientation in each measurement. However, we also wanted to see what the results would look like if we could follow the same spot throughout the crystallization process. For this purpose, we needed to have faster crystallization for practical purposes. Here, amorphous indomethacin was crystallized rapidly with a drop of ethanol. The amorphous sample dissolved partially in the ethanol, and crystallization started from the ethanol solution (solution-mediated crystallization). The whole imaged area was initially wetted with ethanol. In these measurements, the sample was not moved between the measurements, and the fluorescence intensities of the FLIM images were proportional to each other. This meant that the lifetime distributions presenting the average arrival-time distributions of the photons could be used for quantitative measurements.

In this experiment, there were two different areas present in the FLIM images: an area where the time-resolved fluorescence stayed almost unchanged, and an area where the fluorescence lifetime increased. The clearest difference between these two areas was again seen in the fluorescence-lifetime amplitudes (Figure 6a). The time-resolved fluorescence from the stable

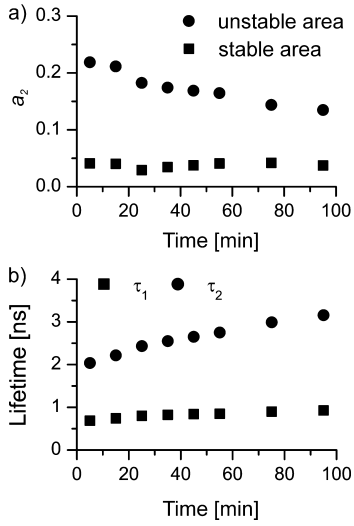


**Figure 6.** (a) Fluorescence-lifetime amplitudes, $a_2$, for the unstable and stable areas of the FLIM images and (b) fluorescence lifetimes, $\tau_1$ and $\tau_2$, for the unstable areas in the FLIM images as a function of time for the ethanol-induced crystallization. The fluorescence lifetimes and their amplitudes were obtained from a biexponential fit to the decay curves extracted from FLIM images.

area was closest to that of pure $\alpha$-indomethacin ($\tau_1$ = 1.15 ns, $a_1$ = 0.96; $\tau_2$ = 3.6 ns, $a_2$ = 0.04). It is known that crystallization in supersaturated ethanol solutions can result in the $\alpha$-form instead of the more stable $\gamma$-form.[38] At $t$ = 5 min, the time-resolved fluorescence extracted from the unstable area of the FLIM image resembled that of amorphous indomethacin ($\tau_1$ = 0.69 ns, $a_1$ = 0.78; $\tau_2$ = 2.0 ns, $a_2$ = 0.22). In reality, the sample consisted of indomethacin in its crystalline and amorphous forms as well as indomethacin dissolved in ethanol. For the analysis, this area was assumed to correspond to amorphous indomethacin. After 95 min, the fluorescence lifetime in the unstable area more closely resembled that of crystalline indomethacin than that of amorphous indomethacin (Figure 6b). The fitting of the decay curves extracted from the whole image area did not give reasonable results because of the multiple fluorescence lifetimes present in the same FLIM image. However, the observed fluorescence-lifetime distribution (Figure 7a) changed uniformly as the crystallization proceeded. With the exception of $t$ = 5 min, the lifetime distributions crossed each other at the isosbestic point at 1.78 ns, indicating the existence of two species contributing to the lifetime distributions. At $t$ = 5 min, there was most probably still a significant amount of indomethacin dissolved in ethanol present in the sample, which would explain why the curve


DOI: 10.1021/acs.molpharmaceut.8b00117
Mol. Pharmaceutics 2018, 15, 1964−1971

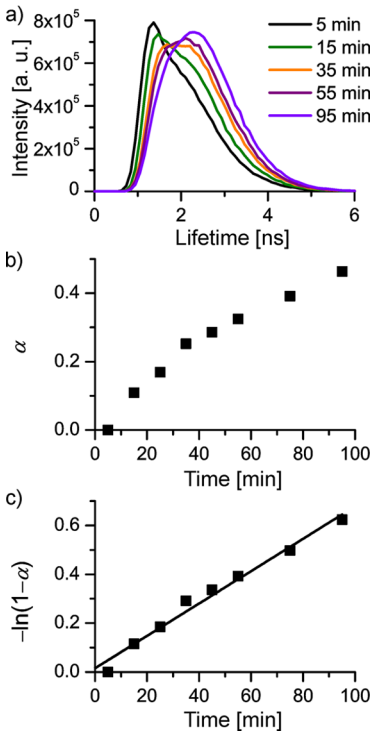


**Figure 7.** (a) Fluorescence-lifetime distributions extracted from the FLIM images of the ethanol-induced crystallization. For clarity, the lifetime distributions for $t$ = 25, 45, and 75 min are not presented. (b) Degree of conversion, $\alpha$, calculated from the lifetime distributions. (c) Fit to the first-order reaction model for the amorphous indomethacin crystallized by ethanol.

does not go through the isosbestic point. The intensity of the band at 1.47 ns was assumed to correspond to the amount of amorphous indomethacin in the sample, and that of the band at 2.21 ns was assumed to correspond to that of crystalline indomethacin. The initial degree of conversion was calculated from the intensities of these bands according to eq 3. Determining the onset of crystallization and the final conversion was not possible from the fluorescence-lifetime distributions. The actual conversion was calculated from the initial conversion, as described in the Experimental Section. It is presented in Figure 7b. The conversion gave a reasonable fit to the first-order reaction model ($R^2$ = 0.977). The fit is presented in Figure 7c. A similar analysis was done to the fluorescence-decay curves extracted from the unstable areas of the FLIM images during the crystallization process, with similar results (not presented).

To detect the fluorescence-lifetime distribution change, as in this example, the crystallization rate of the monitored area should be feasible for detection with the experimental equipment. As one measurement can take up to 5 min, it is not reasonable to try to detect the crystallization rates of the samples that crystallize completely in 5−15 min. The maximum scan area of our equipment was 80 × 80 $\mu$m, and in most of the attempts to monitor the ethanol-induced crystallization, the sample crystallized too fast in the monitored area for kinetic analysis. This can be avoided by using FLIM equipment with a larger scanning area or faster data acquisition. However, our results clearly indicate that it is possible to monitor the crystallization process using FLIM images with several fluorescence lifetimes when the FLIM-image intensities are proportional to each other.

## CONCLUSIONS

We were able to identify different solid indomethacin forms (amorphous and $\gamma$- and $\alpha$-crystalline) and monitor the crystallization of the amorphous form by fluorescence-lifetime-imaging microscopy (FLIM). According to our results, there are two possible approaches for the kinetic analysis of FLIM data. If the crystallization is rapid enough, and there is no need to move the sample during crystallization, the crystallization kinetics can be obtained from a fluorescence-lifetime-distribution analysis. A lifetime-distribution analysis can be used even if there are several different fluorescence lifetimes present in the sample, as presented in this study. The second method for kinetic analysis is to use the fluorescence-lifetime amplitudes calculated from the decay curves for kinetic analysis. Although the fluorescence intensity is sensitive to external factors such as the sample orientation and focal plane, fluorescence lifetimes and their amplitudes are unaffected, as demonstrated during the 10 day monitoring period. This allows the removal of the samples from the equipment between measurements, and the same sample can be monitored quantitatively as long as needed. In future studies, it would be interesting to compare the FLIM method to other imaging techniques, such as Raman, CARS, or FTIR microscopy. In short, we have demonstrated that FLIM is a sensitive and nondestructive method for monitoring crystallization on the surface of a sample.

## AUTHOR INFORMATION

### Corresponding Author

*E-mail: kaisa.rautaniemi@tut.fi. Tel.: +358500225362.

### ORCID

Kaisa Rautaniemi: 0000-0002-8665-4173

Elina Vuorimaa-Laukkanen: 0000-0002-3610-785X

Clare J. Strachan: 0000-0003-3134-8918

Timo Laaksonen: 0000-0002-6699-3004

### Author Contributions

The manuscript was written through contributions of all authors. All authors have given approval to the final version of the manuscript.

### Notes

The authors declare no competing financial interest.

## ACKNOWLEDGMENTS

K.R. and E.V.-L. acknowledge funding from the Academy of Finland (Grant 311362). T.L. acknowledges funding from the Academy of Finland (Grant 258114).

## REFERENCES

(1) Babu, N. J.; Nangia, A. Solubility Advantage of Amorphous Drugs and Pharmaceutical Cocrystals. *Cryst. Growth Des.* **2011**, *11* (7), 2662−2679.

(2) Yu, L. Amorphous Pharmaceutical Solids: Preparation, Characterization and Stabilization. *Adv. Drug Delivery Rev.* **2001**, *48* (1), 27−42.

(3) Démuth, B.; Nagy, Z. K.; Balogh, A.; Vigh, T.; Marosi, G.; Verreck, G.; Van Assche, I.; Brewster, M. E. Downstream Processing of Polymer-Based Amorphous Solid Dispersions to Generate Tablet Formulations. *Int. J. Pharm.* **2015**, *486*, 268−286.

(4) Andronis, V.; Zografi, G. Crystal Nucleation and Growth of Indomethacin Polymorphs from the Amorphous State. *J. Non-Cryst. Solids* **2000**, *271* (3), 236−248.

(5) Andronis, V.; Yoshioka, M.; Zografi, G. Effects of Sorbed Water on the Crystallization of Indomethacin from the Amorphous State. *J. Pharm. Sci.* **1997**, *86* (3), 346−357.



DOI: 10.1021/acs.molpharmaceut.8b00117
*Mol. Pharmaceutics* 2018, 15, 1964−1971

(6) Greco, K.; Bogner, R. Crystallization of Amorphous Indomethacin during Dissolution: Effect of Processing and Annealing. *Mol. Pharmaceutics* **2010**, *7* (5), 1406−1418.
(7) Karmwar, P.; Graeser, K.; Gordon, K. C.; Strachan, C. J.; Rades, T. Investigation of Properties and Recrystallisation Behaviour of Amorphous Indomethacin Samples Prepared by Different Methods. *Int. J. Pharm.* **2011**, *417* (1−2), 94−100.
(8) Wu, T.; Yu, L. Surface Crystallization of Indomethacin below T G. *Pharm. Res.* **2006**, *23* (10), 2350−2355.
(9) Lefort, R.; De Gusseme, A.; Willart, J. F.; Danède, F.; Descamps, M. Solid State NMR and DSC Methods for Quantifying the Amorphous Content in Solid Dosage Forms: An Application to Ball-Milling of Trehalose. *Int. J. Pharm.* **2004**, *280* (1−2), 209−219.
(10) Taylor, L. S.; Zografi, G. The Quantitative Analysis of Crystallinity Using FT-Raman Spectroscopy. *Pharm. Res.* **1998**, *15* (5), 755−761.
(11) Hédoux, A.; Paccou, L.; Guinet, Y.; Willart, J. F.; Descamps, M. Using the Low-Frequency Raman Spectroscopy to Analyze the Crystallization of Amorphous Indomethacin. *Eur. J. Pharm. Sci.* **2009**, *38* (2), 156−164.
(12) Mah, P. T.; Laaksonen, T.; Rades, T.; Aaltonen, J.; Peltonen, L.; Strachan, C. J. Unravelling the Relationship between Degree of Disorder and the Dissolution Behavior of Milled Glibenclamide. *Mol. Pharmaceutics* **2014**, *11* (1), 234−242.
(13) Frenette, M.; Cosa, G.; Friščić, T. Characterisation of Organic Solid Forms and Real-Time in Situ Monitoring of Their Transformations Using Solid-State Fluorescence. *CrystEngComm* **2013**, *15* (25), 5100.
(14) Woltmann, E.; Meyer, H.; Weigel, D.; Pritzke, H.; Posch, T. N.; Kler, P. A.; Schürmann, K.; Roscher, J.; Huhn, C. Applicability of UV Laser-Induced Solid-State Fluorescence Spectroscopy for Characterization of Solid Dosage Forms. *Anal. Bioanal. Chem.* **2014**, *406* (25), 6347−6362.
(15) Alves, J. C. L.; Poppi, R. J. Simultaneous Determination of Acetylsalicylic Acid, Paracetamol and Caffeine Using Solid-Phase Molecular Fluorescence and Parallel Factor Analysis. *Anal. Chim. Acta* **2009**, *642* (1−2), 212−216.
(16) Moreira, A. B.; Dias, I. L. T.; Neto, G. O.; Zagatto, E. A. G.; Kubota, L. T. Solid-Phase Fluorescence Spectroscopy for the Determination of Acetylsalicylic Acid in Powdered Pharmaceutical Samples. *Anal. Chim. Acta* **2004**, *523* (1), 49−52.
(17) Tian, B.; Tang, X.; Taylor, L. S. Investigating the Correlation between Miscibility and Physical Stability of Amorphous Solid Dispersions Using Fluorescence-Based Techniques. Mol. *Mol. Pharmaceutics* **2016**, *13* (11), 3988−4000.
(18) Berezin, M. Y.; Achilefu, S. Fluorescence Lifetime Measurements and Biological Imaging. *Chem. Rev.* **2010**, *110* (5), 2641−2684.
(19) Becker, W. Fluorescence Lifetime Imaging - Techniques and Applications. *J. Microsc.* **2012**, *247* (2), 119−136.
(20) Surwase, S. A.; Boetker, J. P.; Saville, D.; Boyd, B. J.; Gordon, K. C.; Peltonen, L.; Strachan, C. J. Indomethacin: New Polymorphs of an Old Drug. *Mol. Pharmaceutics* **2013**, *10* (12), 4472−4480.
(21) Kaneniwa, N.; Otsuka, M.; Hayashi, T. Physicochemical Characterization of Indomethacin Polymorphs and the Transformation Kinetics in Ethanol. *Chem. Pharm. Bull.* **1985**, *33* (8), 3447−3455.
(22) Lin, S. Y.; Lin, H. L.; Chi, Y. T.; Huang, Y. T.; Kao, C. Y.; Hsieh, W. H. Thermoanalytical and Fourier Transform Infrared Spectral Curve-Fitting Techniques Used to Investigate the Amorphous Indomethacin Formation and Its Physical Stability in Indomethacin-Soluplus® Solid Dispersions. *Int. J. Pharm.* **2015**, *496* (2), 457−465.
(23) Pan, X.; Julian, T.; Augsburger, L. Increasing the Dissolution Rate of a Low-Solubility Drug Through a Crystalline-Amorphous Transition: A Case Study with Indomethicin. *Drug Dev. Ind. Pharm.* **2008**, *34* (2), 221−231.
(24) Savolainen, M.; Heinz, A.; Strachan, C.; Gordon, K. C.; Yliruusi, J.; Rades, T.; Sandler, N. Screening for Differences in the Amorphous State of Indomethacin Using Multivariate Visualization. *Eur. J. Pharm. Sci.* **2007**, *30* (2), 113−123.
(25) Khawam, A.; Flanagan, D. R. Solid-State Kinetic Models: Basics and Mathematical Fundamentals. *J. Phys. Chem. B* **2006**, *110* (35), 17315−17328.
(26) Xiang, T.-X.; Anderson, B. D. Molecular Dynamics Simulation of Amorphous Indomethacin. Mol. *Mol. Pharmaceutics* **2013**, *10* (1), 102−114.
(27) Ghatak, A.; Mandal, P. C.; Sarkar, M. Indomethacin: A NSAID Sensitive to Micro Heterogeneity in Alcohol-Water Mixtures. *Chem. Phys. Lett.* **2008**, *460* (4−6), 521−524.
(28) Maity, B.; Chatterjee, A.; Ahmed, S. A.; Seth, D. Interaction of the Nonsteroidal Anti-Inflammatory Drug Indomethacin with Micelles and Its Release. *J. Phys. Chem. B* **2015**, *119* (9), 3776−3785.
(29) Savolainen, M.; Heinz, A.; Strachan, C.; Gordon, K. C.; Yliruusi, J.; Rades, T.; Sandler, N. Screening for Differences in the Amorphous State of Indomethacin Using Multivariate Visualization. *Eur. J. Pharm. Sci.* **2007**, *30* (2), 113−123.
(30) Hasebe, M.; Musumeci, D.; Powell, C. T.; Cai, T.; Gunn, E.; Zhu, L.; Yu, L. Fast Surface Crystal Growth on Molecular Glasses and Its Termination by the Onset of Fluidity. *J. Phys. Chem. B* **2014**, *118* (27), 7638−7646.
(31) Crowley, K. J.; Zografi, G. Cryogenic Grinding of Indomethacin Polymorphs and Solvates: Assessment of Amorphous Phase Formation and Amorphous Phase Physical Stability. *J. Pharm. Sci.* **2002**, *91* (2), 492−507.
(32) Devlin, J. P.; Gulluru, D. B.; Buch, V. Rates and Mechanisms of Conversion of Ice Nanocrystals to Hydrates of HCl and HBr: Acid Diffusion in the Ionic Hydrates. *J. Phys. Chem. B* **2005**, *109* (8), 3392−3401.
(33) Henning, R. W.; Schultz, A. J.; Thieu, V.; Halpern, Y. Neutron Diffraction Studies of CO2 Clathrate Hydrate: Formation from Deuterated Ice. *J. Phys. Chem. A* **2000**, *104* (21), 5066−5071.
(34) Liu, P.; De Wulf, O.; Laru, J.; Heikkilä, T.; van Veen, B.; Kiesvaara, J.; Hirvonen, J.; Peltonen, L.; Laaksonen, T. Dissolution Studies of Poorly Soluble Drug Nanosuspensions in Non-Sink Conditions. *AAPS PharmSciTech* **2013**, *14* (2), 748−756.
(35) Sun, Y.; Zhu, L.; Kearns, K. L.; Ediger, M. D.; Yu, L. Glasses Crystallize Rapidly at Free Surfaces by Growing Crystals Upward. *Proc. Natl. Acad. Sci. U. S. A.* **2011**, *108* (15), 5990−5995.
(36) Zhu, L.; Jona, J.; Nagapudi, K.; Wu, T. Fast Surface Crystallization of Amorphous Griseofulvin below T G. *Pharm. Res.* **2010**, *27* (8), 1558−1567.
(37) Savolainen, M.; Kogermann, K.; Heinz, A.; Aaltonen, J.; Peltonen, L.; Strachan, C.; Yliruusi, J. Better Understanding of Dissolution Behaviour of Amorphous Drugs by in Situ Solid-State Analysis Using Raman Spectroscopy. *Eur. J. Pharm. Biopharm.* **2009**, *71* (1), 71−79.
(38) Lohani, S.; Nesmelova, I. V.; Suryanarayanan, R.; Grant, D. J. W. Spectroscopic Characterization of Molecular Aggregates in Solutions: Impact on Crystallization of Indomethacin Polymorphs from Acetonitrile and Ethanol. *Cryst. Growth Des.* **2011**, *11* (6), 2368−2378.


DOI: 10.1021/acs.molpharmaceut.8b00117
*Mol. Pharmaceutics* 2018, 15, 1964−1971